Fault Ride Though Control of Photovoltaic Grid-connected Inverter with Current-limited Capability under Offshore Unbalanced Voltage Conditions

Liu, Wenzhao; Guo, Xiaoqiang; Savaghebi, Mehdi; Guerrero, Josep M.

Published in:
Proceedings of Offshore energy & storage symposium 2016

Publication date:
2016

Document Version
Early version, also known as pre-print

Fault Ride Though Control of Photovoltaic Grid-connected Inverter with Current-limited Capability under Offshore Unbalanced Voltage Conditions

Wenzhao Liu*, Xiaoqiang Guo†, Mehdi Savaghebi*, Josep. M Guerrero*

* Department of Energy Technology, Aalborg University, Denmark
† Department of Electrical Engineering, Yanshan University, China
{wzl, mes, joz}@et.aau.dk*, gxq@ysu.edu.cn†
www.microgrids.et.aau.dk

Abstract

The photovoltaic (PV) inverter installed on board experiences the excessive current stress in case of the offshore unbalanced voltage fault ride through (FRT), which significantly affects the operation reliability of the power supply system. In order to solve the problem, the inherent mechanism of the excessive current phenomenon with the conventional fault ride through control is discussed. The quantitative analysis of the current peak value is conducted and a new current-limiting control strategy is proposed to achieve the flexible power control and successful fault ride through in a safe current operation area, which is beneficial to the system reliability. Finally, the simulations of conventional and proposed control solutions are carried out. The results verify the effectiveness of the proposed method.

Keywords: photovoltaic grid-connected inverter, fault ride through, offshore unbalanced grid voltage

1 Introduction

In recent years, offshore microgrids integrated with renewable power source have attracted considerable attentions because of its economic and environmental aspects and flexible controllability[1]. As the interface device connected to the source, loads and offshore grid, the photovoltaic(PV) grid-connected inverters can play an beneficial supplement role to enhance shipboard power quality and ensure the power system ride though short-term disturbances, especially under unbalanced grid voltage conditions[2]. The unbalanced ship grid voltage may be caused by seveal short-circuit faults such as phase-ground or phase-phase faults onboard. However, during the ship grid voltage sag faults, one or more phase voltages at the Point of Common Coupling (PCC) are reduced and the currents supplied by the source must be increased in order to maintain the same amount of injected power in the nominal grid voltage conditions[3]. Further, these overcurrents can damage the operation of high frequency switches of PV inverter as well as the interconnection electric lines, and finally affects the continuty of the whole offshore power supply system [4]. Therefore, it is neccessary to find a solution to solve the above metioned problems.

Advanced FRT control algorithms are proposed based on symmetric sequences to acheive particular control targets related to current harmonic, power oscillations, dc bus ripples and voltage support during the onshore/offshore grid voltage sags conditions[5-9]. However, few works have been developed to decribe fault limitng control cinsidering the shipboard power system. The utilization of Fault Current Limiters (FCLs) to suppress fault currents can result in considerable saving in the investment of high capacity circuit breakers, but FCL impedance required for short circuit current reduction and it is derived with the impedance matrix complex methods [10] The concept of the possibility to use the power converters for fault current limiting and current breaking is described in [11] but this strategy still needs to add extra devices and increase the volume and weight of the ship electrical system. In addition, reference [12] proposed a modular multilevel dual active bridge (M2DAB) converter is proposed to be applied in shipboard system, the bi-directional isolated dc/dc converter with fault protection and ride-through capability can limit the fault current, but it is only applied in the shipboard DC system.

In this paper, a novel current-limited control strategy is presented to achieve the flexible power control and successful FRT in a safe current operation area, which is beneficial to the reliability of ship AC power supply systems.

2 Control strategy

Fig. 1 illustrates the schematic diagram of the PV grid-connected inverter. The DC voltage U_d can be supplied by photovoltaic cells through a DC/DC boost circuit, and the inverter output via LCL filter is connected to shipboard AC grid.

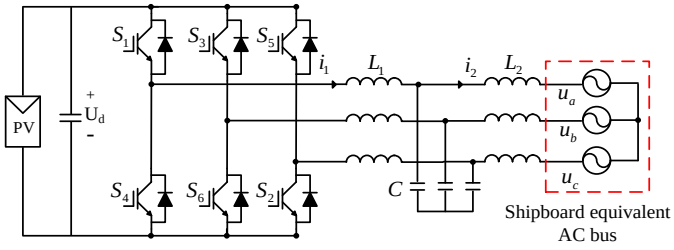

Fig.1. Schematic diagram of grid-connected inverter

A. Quantitative analysis of overcurrent

The three-phase PCC voltage can be expressed as follow

$$\begin{bmatrix} u_a \\ u_b \\ u_c \end{bmatrix} = \begin{bmatrix} U^+ \sin(\omega t + \theta_p) + U^- \sin(\omega t + \theta_n) \\ U^+ \sin(\omega t + \theta_p - 120^\circ) + U^- \sin(\omega t + \theta_n + 120^\circ) \\ U^+ \sin(\omega t + \theta_p + 120^\circ) + U^- \sin(\omega t + \theta_n - 120^\circ) \end{bmatrix} \quad (1)$$

where U^+, U^-, θ_p , θ_n and ω represents the positive and negative sequence voltage amplitude, phase angle and angular frequency respectively.

With the Clarke transformation, equation (1) can be expressed in stationary frame as follows

$$\begin{cases} \begin{bmatrix} u_\alpha \\ u_\beta \end{bmatrix} = \frac{2}{3} \begin{bmatrix} 1 & -\frac{1}{2} & -\frac{1}{2} \\ 0 & \frac{\sqrt{3}}{2} & -\frac{\sqrt{3}}{2} \end{bmatrix} \begin{bmatrix} u_a \\ u_b \\ u_c \end{bmatrix} = \begin{bmatrix} u_\alpha^+ + u_\alpha^- \\ u_\beta^+ + u_\beta^- \end{bmatrix} \\ \begin{bmatrix} u_\alpha^+ \\ u_\beta^+ \end{bmatrix} = \begin{bmatrix} U^+ \sin(\omega t + \theta_p) \\ -U^+ \cos(\omega t + \theta_p) \end{bmatrix} \quad \begin{bmatrix} u_\alpha^- \\ u_\beta^- \end{bmatrix} = \begin{bmatrix} U^- \sin(\omega t + \theta_n) \\ U^- \cos(\omega t + \theta_n) \end{bmatrix} \end{cases} \quad (2)$$

According to instantaneous power theory, the active and reactive output power of the inverter can be expessed as [13]:

$$\begin{bmatrix} p \\ q \end{bmatrix} = \frac{3}{2} \begin{bmatrix} u_\alpha & u_\beta \\ u_\beta & -u_\alpha \end{bmatrix} \begin{bmatrix} i_\alpha \\ i_\beta \end{bmatrix} \quad (3)$$

The output currents of PV inverter can be derived from equation (3) as

$$\begin{bmatrix} i_\alpha \\ i_\beta \end{bmatrix} = \frac{2}{3} \begin{bmatrix} u_\alpha & u_\beta \\ u_\beta & -u_\alpha \end{bmatrix}^{-1} \begin{bmatrix} P^* \\ Q^* \end{bmatrix} = \begin{bmatrix} i_{\alpha(p)} + i_{\alpha(q)} \\ i_{\beta(p)} + i_{\beta(q)} \end{bmatrix} \quad (4)$$

where $P^*$and Q^* are the inverter output active and reactive power reference and detemined by the inverter rated capacity. $i_{\alpha(p)}, i_{\beta(p)}, i_{\alpha(q)}$ and $i_{\beta(q)}$ represent the active and reactive power current components in stationary frame respectively. Thus, equation (4) can be refermulated as follows

$$\begin{bmatrix} i_\alpha \\ i_\beta \end{bmatrix} = \begin{bmatrix} i_{\alpha(p)} \\ i_{\beta(p)} \end{bmatrix} + \begin{bmatrix} i_{\alpha(q)} \\ i_{\beta(q)} \end{bmatrix} = \frac{2}{3} \frac{P^*}{u_\alpha^2 + u_\beta^2} \begin{bmatrix} u_\alpha \\ u_\beta \end{bmatrix} + \frac{2}{3} \frac{Q^*}{u_\alpha^2 + u_\beta^2} \begin{bmatrix} u_\beta \\ -u_\alpha \end{bmatrix} \quad (5)$$

Substituting (2) into (5) the currentcomponents can be obtained as follows

$$\begin{cases} \begin{bmatrix} i_{\alpha(p)} \\ i_{\beta(p)} \end{bmatrix} = \frac{2}{3} \frac{P^*}{(u_\alpha^+ + u_\alpha^-)^2 + (u_\beta^+ + u_\beta^-)^2} \begin{bmatrix} u_\alpha^+ + u_\alpha^- \\ u_\beta^+ + u_\beta^- \end{bmatrix} \\ \begin{bmatrix} i_{\alpha(q)} \\ i_{\beta(q)} \end{bmatrix} = \frac{2}{3} \frac{Q^*}{(u_\alpha^+ + u_\alpha^-)^2 + (u_\beta^+ + u_\beta^-)^2} \begin{bmatrix} u_\beta^+ + u_\beta^- \\ -u_\alpha^+ - u_\alpha^- \end{bmatrix} \end{cases} \quad (6)$$

In order to realize the flexible power control during the FRT process, the adjustable coefficients k_p and k_q are introduced in (6) and the output current referenece can be rewritten as follows

$$\begin{cases} i_{\alpha(p)} = \frac{2}{3} \frac{P^*}{[(u_\alpha^+)^2 + (u_\beta^+)^2] + k_p[(u_\alpha^-)^2 + (u_\beta^-)^2]} [(u_\alpha^+) + (k_p u_\alpha^-)] \\ i_{\beta(p)} = \frac{2}{3} \frac{P^*}{[(u_\alpha^+)^2 + (u_\beta^+)^2] + k_p[(u_\alpha^-)^2 + (u_\beta^-)^2]} [(u_\beta^+) + (k_p u_\beta^-)] \\ i_{\alpha(q)} = \frac{2}{3} \frac{Q^*}{[(u_\alpha^+)^2 + (u_\beta^+)^2] + k_q[(u_\alpha^-)^2 + (u_\beta^-)^2]} [(u_\beta^+) + (k_q u_\beta^-)] \\ i_{\beta(q)} = \frac{2}{3} \frac{Q^*}{[(u_\alpha^+)^2 + (u_\beta^+)^2] + k_q[(u_\alpha^-)^2 + (u_\beta^-)^2]} [-(u_\alpha^+) - (k_q u_\alpha^-)] \end{cases} \quad (7)$$

It should be noted that k_p and k_q meet the requirement equation $k_p+k_q=0$. There are special conditions for this control strategy. In particular, when $k_p=-1$, $k_q=1$ the control stragety can be realized for constant active power control, $k_p = 1$, $k_q = -1$ as for the constant reactive power control, $k_p = k_q = 0$ is for the balanced current control, and k_p and k_q changes within the range [-1, 1] to realize flexible power control [14]. However, all of these control targets exits the excessive current stress, which would significantly affect the operation reliability of power supply system.

The following will present a quantitative analysis of inverter overcurrent. Substituting (2) into (7) and simplifying the equation to obtain the active and reactive power currents

$$\begin{cases} I_{\alpha(p)} = \frac{2}{3} \frac{P^*}{[(U^+)^2 + k_p(U^-)^2]} [U^+ \sin(\omega t + \theta_\mathbf{p}) + k_p U^- \sin(\omega t + \theta_\mathbf{n})] \\ I_{\beta(p)} = \frac{2}{3} \frac{P^*}{[(U^+)^2 + k_p(U^-)^2]} [-U^+ \cos(\omega t + \theta_\mathbf{p}) + k_p U^- \cos(\omega t + \theta_\mathbf{n})] \\ I_{\alpha(q)} = \frac{2}{3} \frac{Q^*}{[(U^+)^2 + k_q(U^-)^2]} [-U^+ \cos(\omega t + \theta_\mathbf{p}) + k_q U^- \cos(\omega t + \theta_\mathbf{n})] \\ I_{\beta(q)} = \frac{2}{3} \frac{Q^*}{[(U^+)^2 + k_q(U^-)^2]} [-U^+ \sin(\omega t + \theta_\mathbf{p}) - k_q U^- \sin(\omega t + \theta_\mathbf{n})] \end{cases} \quad (8)$$

The current reference in the stationary frame can be expressed as follows

$$\begin{aligned} \begin{bmatrix} I_\alpha^* \\ I_\beta^* \end{bmatrix} &= \begin{bmatrix} I_{\alpha(p)} + I_{\alpha(q)} \\ I_{\beta(p)} + I_{\beta(q)} \end{bmatrix} \\ &= \frac{2}{3} \begin{bmatrix} \mathrm{A}_1 \sin(\omega t + \theta_\mathrm{p} - \delta_1) + \mathrm{A}_2 \sin(\omega t + \theta_\mathrm{n} + \delta_2) \\ -\mathrm{A}_1 \cos(\omega t + \theta_\mathrm{p} - \delta_1) + \mathrm{A}_2 \cos(\omega t + \theta_\mathrm{n} + \delta_2) \end{bmatrix} \end{aligned} \quad (9)$$

where

$$\mathrm{A}_1 = \sqrt{\left[\frac{U^+ P^*}{(U^+)^2 + k_p(U^-)^2}\right]^2 + \left[\frac{U^+ Q^*}{(U^+)^2 + k_q(U^-)^2}\right]^2}$$

$$\delta_1 = \mathrm{atan} \frac{Q^*[(U^+)^2 + k_p(U^-)^2]}{P^*[(U^+)^2 + k_q(U^-)^2]}$$

$$\mathrm{A}_2 = \sqrt{\left[\frac{k_p U^- P^*}{(U^+)^2 + k_p(U^-)^2}\right]^2 + \left[\frac{k_q U^- Q^*}{(U^+)^2 + k_q(U^-)^2}\right]^2} ,$$

$$\delta_2=\text{atan}\frac{k_q Q^*[(U^+)^2+k_p(U^-)^2]}{k_p P^*[(U^+)^2+k_q(U^-)^2]}.$$

With the inverse Clarke transformation, equation (9) can be expressed in abc frame as follows

$$\begin{bmatrix} I_a^* \\ I_b^* \\ I_c^* \end{bmatrix}=\frac{2}{3}\begin{bmatrix} \sqrt{A_1^2+A_2^2-2A_1A_2\cos(\theta_p-\delta_1-\theta_n-\delta_2)}\sin(\omega t+\psi_a) \\ \sqrt{A_1^2+A_2^2-2A_1A_2\cos(\theta_p-\delta_1-\theta_n-\delta_2-240^\circ)}\sin(\omega t+\psi_b) \\ \sqrt{A_1^2+A_2^2-2A_1A_2\cos(\theta_p-\delta_1-\theta_n-\delta_2+240^\circ)}\sin(\omega t+\psi_c) \end{bmatrix} \tag{10}$$

where

$$\psi_a=\text{atan}\frac{A_1\sin(\theta_p-\delta_1)-A_2\sin(\theta_n+\delta_2)}{A_1\cos(\theta_p-\delta_1)-A_2\cos(\theta_n+\delta_2)},$$

$$\psi_b=\text{atan}\frac{A_1\sin(\theta_p-\delta_1-120^\circ)-A_2\sin(\theta_n+\delta_2+120^\circ)}{A_1\cos(\theta_p-\delta_1-120^\circ)-A_2\cos(\theta_n+\delta_2+120^\circ)},$$

$$\psi_c=\text{atan}\frac{A_1\sin(\theta_p-\delta_1+120^\circ)-A_2\sin(\theta_n+\delta_2-120^\circ)}{A_1\cos(\theta_p-\delta_1+120^\circ)-A_2\cos(\theta_n+\delta_2-120^\circ)}.$$

The peak value of the inverter output current can be obtained from (10) as follow

$$I_{\max}^*=\frac{2}{3}(A_1+A_2)=\frac{2}{3}\sqrt{\left[\frac{U^+P^*}{(U^+)^2+k_p(U^-)^2}\right]^2+\left[\frac{U^+Q^*}{(U^+)^2+k_q(U^-)^2}\right]^2}+\frac{2}{3}\sqrt{\left[\frac{k_pU^-P^*}{(U^+)^2+k_p(U^-)^2}\right]^2+\left[\frac{k_qU^-Q^*}{(U^+)^2+k_q(U^-)^2}\right]^2} \tag{11}$$

It should be noted that when the ship grid voltage is balanced which means negative sequence voltage $U^-=0$, three phase inverter output current peak value is expressed as (12) which is consistent with reference [15]:

$$I_{\max-\text{balance}}^*=\frac{2\sqrt{(P^*)^2+(Q^*)^2}}{3U^+} \tag{12}$$

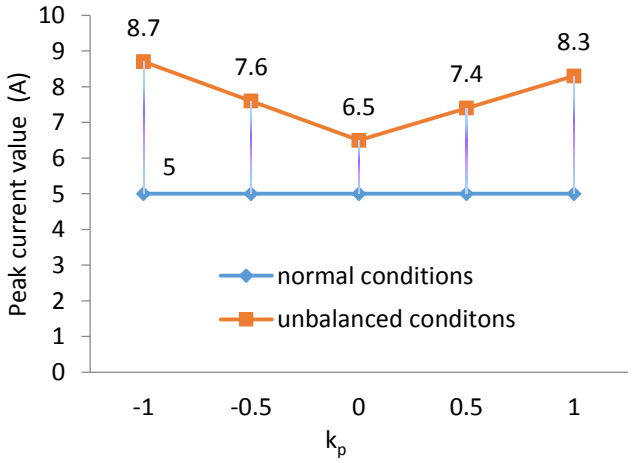

Fig.2. Current peak value computation results with different k_p under unbalanced and normal conditions

On the other hand, if the ship grid voltage is unbalanced ($U^-\neq 0$), there are always excess current outputs in the system no matter how to adjust coefficient k_p and k_q. Furthermore, with the system parameters listed in Table II, the current peak value can be calculated from (11) and (12) under unbalanced and normal conditions and the computation result are shown in Fig.2.

Moreover, in order to achieve unit power factor and constant active power output control, the reactive power can be set as $Q^*=0$ and k_p=-1 k_q=1. Thus, the current peak value can be derived from (11) and (12) under normal ship grid voltage and unbalanced conditions respectively, which are expressed as (13) and (14)

$$I_{\max\text{-normal}}^*=\frac{2P^*}{3U^+} \tag{13}$$

$$I_{\max\text{-unbalance}}^*=\frac{2P^*}{3(U^+-U^-)} \tag{14}$$

Based on the above analysis, it can be observed that the inverter output current peak values under unbalanced conditions are always higher than normal conditions because of the negative sequence voltage component U^-. Therefore, the current should be limited into a safe operation area. The following will present a solution to the PV grid-connected inverter to ensure current-limited operation.

B. ***Proposed current-limited control strategy***

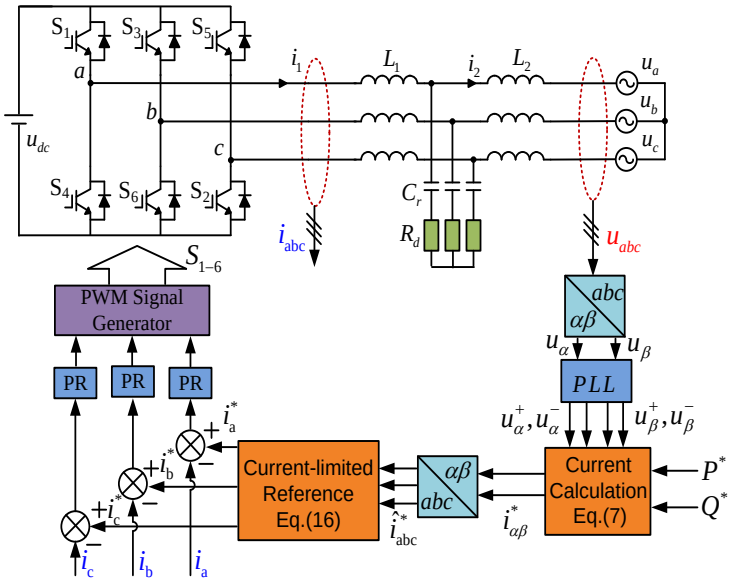

Fig.3. Structure diagram of the proposed current-limited control strategy

The proposed control structure is shown in Fig.3, where R_d is used to damp the potential resonance from LCL filter. The optimization of damping resister is in [16].The Proportional Resonant (PR) controllers are applied to track the alternative current reference precisely with zero steady-state error in a single current closed-loop control [17].

As it can be observed in Fig.3, the ship PCC voltage u_{abc} and PV inverter output current i_{abc} are sampled. With the Clarke transformation, the voltage can be expressed as u_α and u_β,

which are sending to PLL to obtain the positive and negative sequence component $u^{+}_{\alpha\beta}$, $u^{-}_{\alpha\beta}$ [18]. Then, the current reference $i^{*}_{\alpha\beta}$ can be generated with equation (7) by using the active and reactive currents $i_{\alpha(p)}, i_{\beta(p)}, i_{\alpha(q)}, i_{\beta(q)}$ and active/reactive power reference P^{*}, Q^{*}. By substituting (7) into Clarke inverse transform, the actual output current are obtained as follows

$$\begin{bmatrix} \hat{i}_a \\ \hat{i}_b \\ \hat{i}_c \end{bmatrix} = \begin{bmatrix} i_{\alpha(p)}+i_{\alpha(q)} \\ -(i_{\alpha(p)}+i_{\alpha(q)})/2+\sqrt{3}(i_{\beta(p)}+i_{\beta(q)})/2 \\ -(i_{\alpha(p)}+i_{\alpha(q)})/2-\sqrt{3}(i_{\beta(p)}+i_{\beta(q)})/2 \end{bmatrix} \quad (15)$$

In order to limit the output current within a rated operating range during the FRT process of the PV inverter, the current reference based on (15) can be modified to equation (16).

$$\begin{bmatrix} i^{*}_a \\ i^{*}_b \\ i^{*}_c \end{bmatrix} = \frac{I_{\text{rated}}}{I_{\max}} \begin{bmatrix} i_{\alpha(p)}+i_{\alpha(q)} \\ -(i_{\alpha(p)}+i_{\alpha(q)})/2+\sqrt{3}(i_{\beta(p)}+i_{\beta(q)})/2 \\ -(i_{\alpha(p)}+i_{\alpha(q)})/2-\sqrt{3}(i_{\beta(p)}+i_{\beta(q)})/2 \end{bmatrix} \quad (16)$$

where $I_{\max}$ and I_{rated} are the max current peak value and rated peak current value respectively.

Considering the unbalanced grid voltage conditions with the system parameters listed in Table II, the inverter rated output current I_{rated} can be set as 5A for normal conditions. It is clear that the current reference peak value in equation (16) will not beyond I_{rated} no matter how to adjust k_p. The current peak value computation results are shown in Table. I

Table. I System operating states and current peak value

Operation states	*Adjust coefficient*	*Current peak value*
Normal	$k_p, k_q \in [-1,1]$	5.0 A
Unbalanced	$k_p=-1$, $k_q=1$	5.0 A
	$k_p=-0.5$, $k_q=0.5$	5.0 A
	$k_p=0$, $k_q=0$	5.0 A
	$k_p=0.5$, $k_q=-0.5$	5.0 A
	$k_p=1$, $k_q=-1$	5.0 A

3 Simulation results

Table. II System parameters

parameters	*value*	*parameters*	*value*
u_{dc}/V	120	u_a/V	$50\angle 0°$
u_b/V	$34.2\angle -137°$	u_c/V	$34.2\angle 137°$
U^{+}/V	38.5	U^{-}/V	11.5
P^{*}/W	300	Q^{*}/var	225
L_1/mH	5	L_2/mH	1
C/μF	9.9	R_d/Ω	5

In order to verify the effectiveness of the proposed control strategy, the MATLAB/Simulink simulation test are carried on the conventional fault ride through control method and proposed control strategy. It is assumed that the rated current of inverter is 5A and the unbalanced grid voltage fault occurs at 0.15s as shown in Fig.4, k_p is adjusted from -1 to 1, the other system parameters are shown in Table. II.

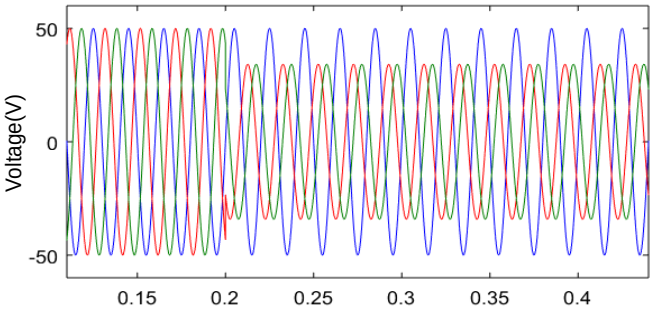

Fig.4 Ship AC bus voltage

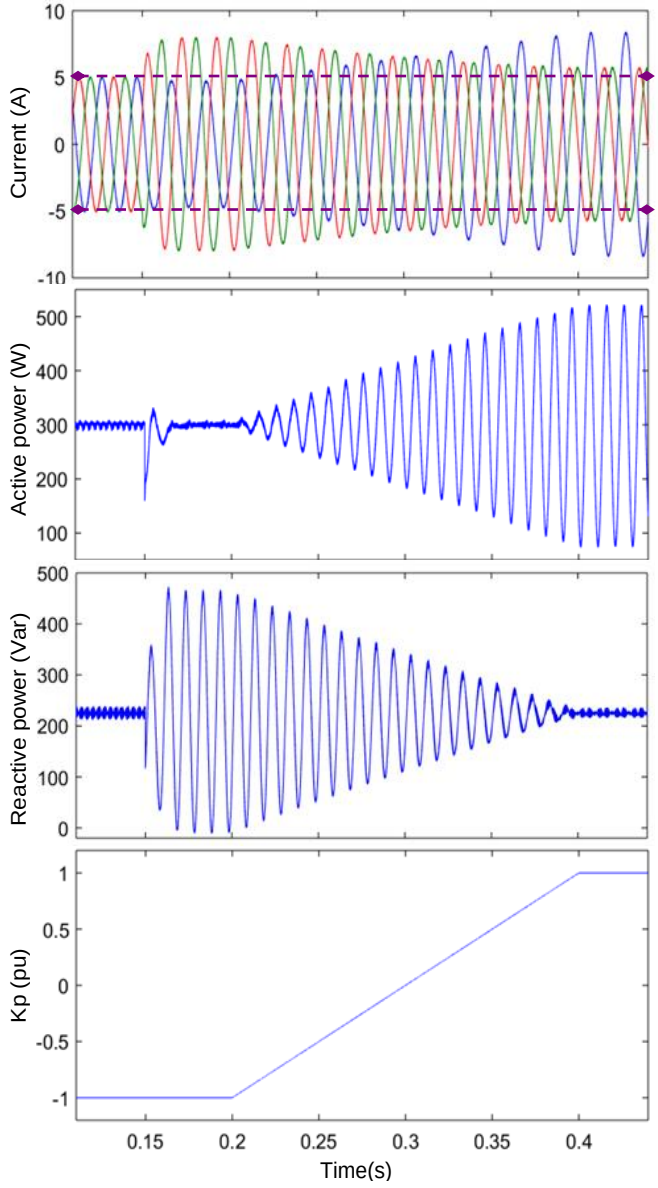

Fig.5 Traditional control strategy

Figure.5 shows the simulation results of traditional fault ride through control with the increasing coefficient k_p. It is can be observed that the inverter output current peak value far more

than the rated current value 5A after the unbalanced grid faults, and the maximum value correctly matches the theoretical calculation results in Fig.2. However, the active and reactive power fluctuations can be regulated with different k_p for some specific applications which are sensitive to power oscillations [15].

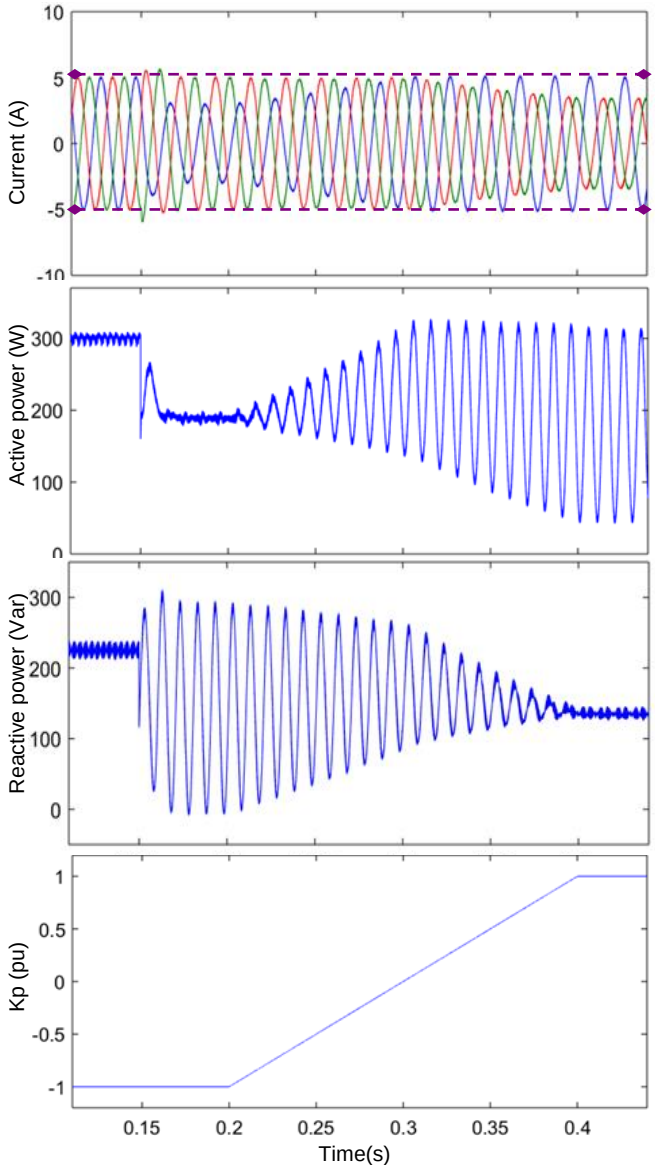

Fig.6 Proposed control strategy

Fig.6 shows the proposed control strategy simulation results. It can be seen that the inverter output current can be limited in 5A rated range by the proposed current-limited control and flexible active and reactive power regulation during the unbalanced grid voltage faults is realized. On the other hand, it should be noted that the performance evaluation are carried out in grid-connected mode of inverter. For islanded mode with unbalanced loads, the proposed method is still valid, but a slight modification is needed to replace the current control with droop control [19]. The detailed analysis and experimental results would be reported in the future.

4 Conclusion

In this paper, the following conclusions can be found through theoretical analysis and simulation research:

1) During the process of unbalanced fault ride through control, the traditional PV grid-connected inverter control scheme will lead to the overcurrent phenomenon and seriously affect the offshore system reliability.

2) The proposed current-limited control strategy can be applied to offshore power supply systems to achieve the flexible power control and successful fault ride through in a safe current operation area under both normal and unbalanced grid voltage conditions.

References

[1] Guerrero, J. M., Vasquez, J. C., Matas, J. Hierarchical control of droop-controlled AC and DC microgrids—A general approach toward standardization. Industrial Electronics, IEEE Transactions on, 2011,58(1), 158-172.

[2] Castilla, M., Miret, J., Camacho, A. Reduction of current harmonic distortion in three-phase grid-connected photovoltaic inverters via resonant current control. Industrial Electronics, IEEE Transactions on, 2013, 60(4), 1464-1472.

[3] Bollen, M. H., & Zhang, L. D. Different methods for classification of three-phase unbalanced voltage dips due to faults. Electric power systems research,2003, 66(1), 59-69.

[4] J.Keller，B.Kroposki Understanding fault characteristics of inverter-based distributed energy resources. NREL/TP-550-46698，National Renewable Energy Laboratory，USA，2010

[5] Daniel Roiu, Radu Iustin Bojoi, Leonardo Rodrigues Limongi, et al. New Stationary Frame Control Scheme for Three-Phase PWM Rectifiers Under Unbalanced Voltage Dips Conditions, IEEE Transactions on Industry Application, 2010, 46(1): 268-277.

[6] Y. Suh and T. A. Lipo. A control scheme in hybrid synchronous-stationary frame for PWM AC/DC converter under generalized unbalanced operating conditions, IEEE Transactions on Industry Application, 2006,42(3): 825-835.

[7] Zixin Li, Yaohua Li, Ping Wang, et al. Control of Three-Phase Boost-Type PWM Rectifier in Stationary Frame Under Unbalanced Input Voltage, IEEE Transactions on Power Electronics, 2010, 25(10): 2521-2530

[8] P. Rodriguez, R. Teodorescu, I. Candela, et al. New Positive-sequence Voltage Detector for Grid Synchronization of Power Converters under Faulty Grid Conditions, IEEE Power Electronics Specialists Conference, South Korea, 2006: 1-7

[9] Rodriguez, P., Timbus, A. V., Teodorescu, R., Flexible active power control of distributed power generation systems during grid faults. Industrial Electronics, IEEE Transactions on, 2007, 54(5), 2583-2592.

[10] Su CL, Su CY, Lee CC, Chen CJ. Fault current limiter allocation in electric ship power systems. InElectric Ship Technologies Symposium, 2009. ESTS 2009. IEEE 2009 Apr 20 pp. 53-58.

[11] Q. Deng, X. Liu, M. Steurer, R. Dougal, and R.R. Soman, "Primary and Backup Protection for MVDC Shipboard Power System", in Proc. of the Electric Ship Technology Symposium, June 22-24, 2015.

[12] Xie R, Shi Y, Li H. Modular multilevel DAB (M 2 DAB) converter for shipboard MVDC system with fault protection and ride-through capability. InElectric Ship Technologies Symposium (ESTS), 2015 IEEE 2015 Jun 21. pp. 427-432

[13] Akagi, Hirofumi, Edson Hirokazu Watanabe, and Mauricio Aredes. "Instantaneous power theory and applications to power conditioning." Vol. 31. John Wiley & Sons, 2007.

[14] Antonio Camacho, Miguel Castilla, Jaume Miret, et al. Flexible Voltage Support Control for Three Phase Distributed Generation Inverters Under Grid Fault, IEEE Transactions on Industrial Electronics, 2013, 60(4): 1429-1441.

[15] Jaume Miret, Miguel Castilla, Antonio Camacho, et al. Control scheme for photovoltaic three-phase inverters to minimize peak currents during unbalanced grid-voltage sags. IEEE Transactions on Power Electronics，2012，27(10)：4262-4271

[16] Pena-Alzola, R., Liserre, M., Blaabjerg, F. Analysis of the passive damping losses in LCL-filter-based grid converters. Power Electronics, IEEE Transactions on, 2013, 28(6), 2642-2646.

[17] Vidal, A., Freijedo, F. D., Yepes, A, Fernandez-Comesana, P., Malvar, J., Lopez, O. Doval-Gandoy, J. Assessment and optimization of the transient response of proportional-resonant current controllers for distributed power generation systems.Industrial Electronics, IEEE Transactions on, 2013, 60(4), 1367-1383.

[18] Guo, X., Wu, W., and Chen, Z. Multiple-complex coefficient-filter-based phase-locked loop and synchronization technique for three-phase grid-interfaced converters in distributed utility networks. Industrial Electronics, IEEE Transactions on, 2011, 58(4), 1194-1204.

[19] De Brabandere, K., Bolsens, B., Van den Keybus, J..A voltage and frequency droop control method for parallel inverters. Power Electronics, IEEE Transactions on, 2007,22(4), 1107-1115.